RESEARCH ARTICLE | JANUARY 07 2025

Ghost imaging through complex scattering media with random light disturbance

Yang Peng ; Wen Chen

Appl. Phys. Lett. 126, 011108 (2025)
https://doi.org/10.1063/5.0252090

Applied Physics Letters ARTICLE pubs.aip.org/aip/apl

Ghost imaging through complex scattering media with random light disturbance

Cite as: Appl. Phys. Lett. **126**, 011108 (2025); doi: 10.1063/5.0252090
Submitted: 7 December 2024 · Accepted: 23 December 2024 ·
Published Online: 7 January 2025

Yang Peng[1] and Wen Chen[1,2,a)]

AFFILIATIONS

[1]Department of Electrical and Electronic Engineering, The Hong Kong Polytechnic University, Hong Kong, China
[2]Photonics Research Institute, The Hong Kong Polytechnic University, Hong Kong, China

[a)]Author to whom correspondence should be addressed: owen.chen@polyu.edu.hk

ABSTRACT

Imaging in a complex environment is recognized to be challenging in various applications. Imaging with single-pixel detection, e.g., ghost imaging (GI), emerges as a solution in recent years. Here, we report a unified GI framework based on untrained neural networks (UNNs) to eliminate the effect of complex environments and realize high-resolution object reconstruction. Two UNNs are designed to respectively estimate the corrected realizations and a series of dynamic scaling factors from the collected realizations. A GI-formation-based physical model is incorporated into the network to ensure the validity of the corrected realizations and enable object reconstruction. Experimental results demonstrate that the proposed method is effective and robust for high-resolution and high-contrast object reconstruction in complex environments, i.e., dynamic scattering media with high-randomness light disturbance. In addition, the proposed method is validated at low sampling ratios to alleviate data acquisition burden. With the advantages in the integration, adaptability, and efficiency, the proposed method provides a promising solution for GI in complex environments.

Ghost imaging (GI) is an innovative technique that has garnered increasing attention over the past decades.[1,2] Unlike traditional imaging that relies on the pixelated detectors, GI can be applied to reconstruct an object by correlating a series of illumination patterns with synchronized realizations captured by a single-pixel detector (SPD).[3,4] Due to the inherent properties of SPD, GI offers low cost and high detection sensitivity. Therefore, GI is particularly suitable for applications in low-light scenarios,[5–7] e.g., imaging through scattering media,[5] biomedical imaging,[6] and long-distance imaging.[7] Additionally, GI has demonstrated potential in the fields of spectroscopy,[8] communication,[9] cryptography,[10] etc.

While existing studies demonstrate the effectiveness of GI in static environments,[11,12] it remains a pivotal concern to maintain the superior performance of GI in dynamic scattering environments. In static environments, constant scaling factors are imposed on the realizations. The introduced effect can be eliminated after a normalization without affecting reconstruction quality. However, real-world scenarios (e.g., underwater and light disturbance) could be dynamic and intricate, resulting in a nonlinear variation of scaling factors and a failure of GI methods.[13] Recently, a temporal correction method[14] was proposed to solve the problem of GI reconstruction in dynamic environments. Although the method has been effective, it demands to double the acquisition time. This limitation has inspired an alternative learning-based correction method,[15] which involves designing a dataset with a specific scaling factor variation. However, scaling factor variations in real-world scenarios are typically unknown or too complex to be explicitly modeled. Consequently, such a supervised paradigm exhibits the limited generalization in its adaptability to environments. To overcome the challenge, an adaptive moving average method[16] was reported to correct scaling factors by exploiting temporal information among neighboring realizations from a statistical perspective. The method could not handle frequent or abrupt scaling factor variations and requires an extra strategy to obtain high-contrast object reconstruction. Contrary to previous methods, here we set our sights on exploring a more efficient and extensive GI framework based on untrained neural networks (UNNs)[17–19] in complex environments with high-randomness light disturbance.

In this Letter, we report a unified GI framework to realize high-resolution and high-contrast object reconstruction in complex environments without requiring datasets in deep learning models. The proposed framework decomposes the realizations collected in complex environments into corrected realizations and scaling factors. Two UNNs are respectively deployed to predict two components through a joint UNN optimization. One network is designed to capture the statistics of latent object information, following a GI-formation-based physical model to estimate the corrected realizations. Another network is adopted to estimate random scaling factor variations. Each scaling factor is predicted independently, without considering temporally adjacent information or depending on explicit assumptions about the scaling factor variation. Experimental results demonstrate that the proposed method can robustly and flexibly reconstruct high-contrast and high-resolution objects in complex environments with high-randomness light disturbance.

In GI, an unknown object $O(x, y)$ is sequentially illuminated by a series of random patterns $P(x, y)$. The realizations captured by the SPD can be used to reconstruct the object with a second-order correlation algorithm, e.g., differential GI (DGI).[4] However, when wave propagation is distorted by a stochastically complex environment, dynamic scaling factors, K, are introduced. The collected realizations $\tilde{B}$ in complex environments can be described by

$$\tilde{B}_i = K_i \iint P_i(x, y) \odot O(x, y)dxdy, \quad (1)$$

where $i = 1, 2, \ldots, N$, N denotes the total number of realizations, and $\odot$ denotes an element-wise multiplication. The stochastic variation of dynamic scaling factors K could be unpredictable and temporally uncorrelated in complex environments. With the presence of the factors K, the correlation between random patterns P and the realizations $\tilde{B}$ is disrupted, impeding the efficacy of conventional GI methods.

The removal of dynamic scaling factors from the collected realizations can be seen as an ill-posed inverse problem to be solved with optimization-based methods. A unified framework that combines two neural networks Ψ_o and Ψ_k is developed to respectively estimate corrected realizations B and scaling factors K. A flow chart of the proposed method is shown in Fig. 1. The network Ψ_o with a uniform-distributed input z_o is adopted to predict B. However, the estimates B would be invalid for object reconstruction without explicit constraints. To address this, instead of directly generating B through the network, Ψ_o is optimized to generate an output to be close to object information $O(x, y) = \Psi_o(z_o)$. Here, $O(x, y)$ is subsequently fed into a GI-formation-based physical model to generate a series of corrected realizations B. The physical model is incorporated into the network using a single convolution layer. The convolution kernel is substituted by a series of random patterns. The weights of convolution kernel correspond to pixel values of random patterns, and the number of kernel channels is equal to the number of random patterns, i.e., N. Therefore, a series of corrected realizations B are generated and formed as a column vector with N entries. To estimate dynamic scaling factors induced by a complex environment, the network Ψ_k is used with an input z_k sampled from the uniform distribution. The input and output dimensions of Ψ_k are determined by the number of random patterns, denoted as $\sqrt{N} \times \sqrt{N}$. The generated two-dimensional matrix is reshaped into a column vector with N entries. The architecture of the individual neural network is an autoencoder with skip connections.[17]

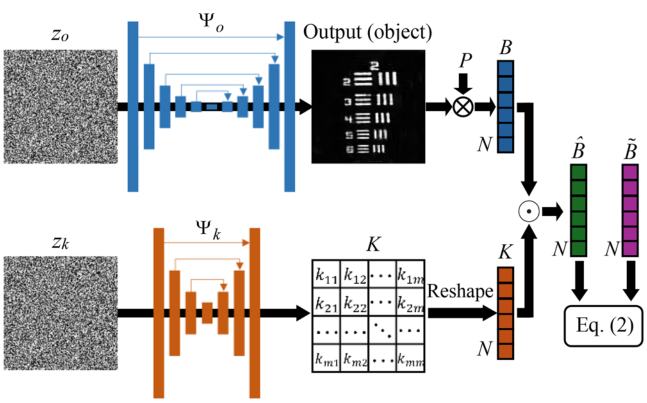

FIG. 1. Flowchart of the developed unified GI framework using UNN in complex environments: $\otimes$, a single convolution layer; k_{mm}, scaling factors; and $m = \sqrt{N}$. Corrected realizations B can be close to those collected in free space without scattering.

With the networks Ψ_o and Ψ_k, estimated realizations $\hat{B} = K \odot B$ can be calculated. The developed unified GI framework in complex environments can be described by

$$\min_{\Psi_o, \Psi_k} \|\Psi_k(z_k) \odot [\Psi_o(z_o) \otimes P] - \tilde{B}\|^2. \quad (2)$$

The parameters of Ψ_o and Ψ_k are jointly updated using the ADAM optimizer on a NVIDIA GeForce RTX 4090 GPU. The learning rate is 0.001. It can be found that an optimal configuration for two networks is realized after the joint UNN optimization. The network Ψ_o is forced to output a high-resolution reconstructed object and subsequently yield the realizations based on the GI-formation-based physical model. The generated corrected realizations are then multiplied by scaling factors generated by Ψ_k to spawn the realizations $\hat{B}$ to be close to the experimentally collected realizations $\tilde{B}$.

To verify the proposed method, a series of optical experiments are conducted in complex environments. In Fig. 2, a green laser beam (MGI-III-532-50mW) is expanded and collimated to illuminate an amplitude-only spatial light modulator (SLM) (Holoeye, LC-R720). 16 384 random patterns with 128×128 pixels are sequentially displayed by SLM. These illumination patterns are magnified by a factor of 2 with a $4f$ optical system and projected onto an object. The complex environment is constructed by using dynamic and turbid water with high-randomness light disturbance. A LED is placed 36.0 cm above the object, providing an illuminance of 10.25 lux. The initial position of the LED corresponds to a rotation angle of 0°, as shown in Fig. 2. In this case, the light area covered by the LED has a diameter of

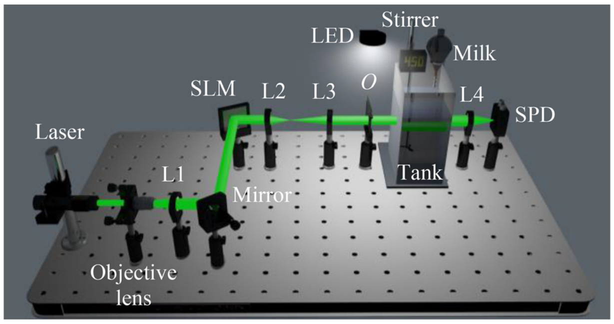

FIG. 2. A schematic experimental setup in complex environments. L1: a collimated lens with a focal length of 10.0 cm; L2: a lens with a focal length of 5.0 cm; L3: a lens with a focal length of 10.0 cm; L4: a lens with a focal length of 5.0 cm; SLM: spatial light modulator; SPD: single-pixel detector; O: object.

approximately 2.2 m. To produce high-randomness light disturbance, the LED is manually rotated in a random manner to various angles between $-90°$ and $40°$ during experiments, with the positive direction defined as rightward. Unknown intensity amplifications could be introduced into the collected realizations at any moment. For dynamic scattering media, 10-ml skimmed milk diluted with 250-ml clean water is continuously dripped into water tank during experiments, and a stirrer works at 450 revolutions per minute to accelerate the mixing of milk and water. The transparent water tank has dimensions of 10.0 cm (length) $\times$ 15.0 cm (width) $\times$ 30.0 cm (height), and an axial distance is 7.0 cm between the front face of the tank and the object. 3000-ml clean water is initially placed in the water tank. A series of light intensities distorted by a complex environment are sequentially collected by the SPD (Thorlabs, PDA100A2), positioned 30.0 cm away from the object.

Figure 3 shows experimental results using a USAF 1951 resolution test chart as an object, when the proposed method in complex environments is applied. To quantitatively evaluate the reconstruction quality, contrast-to-noise ratio (CNR)[20] is calculated [see Eq. (S1) in the supplementary material for details]. In Fig. 3(a), experimentally collected single-pixel intensities exhibit stochastic fluctuations due to the combined effect of scattering and light disturbance. Based on the data in Fig. 3(a), a reconstructed object using conventional DGI is filled with noise and the CNR value is -0.05, as shown in Fig. 3(e). It is indicated that the collected realizations lose effectiveness in ghost reconstruction owing to the influence of complex environments. The proposed method can eliminate the impact of complex environments by separating dynamic scaling factors from the collected realizations. The two designed networks respectively produce corrected realizations in Fig. 3(b) and dynamic scaling factors in Fig. 3(c). The corrected realizations that the network generates uniformly fluctuate and are not affected by complex environments. Dynamic scaling factors, on the contrary, exactly reproduce the influence of complex environments on the collected realizations. Estimated intensities $\hat{B}$ in Fig. 3(d) are derived from a multiplication of these two components and show a high resemblance to the collected intensities $\tilde{B}$, illustrating the effectiveness of the developed joint optimization. Using a constraint with the GI-formation-based physical model, the latent object information is reconstructed with high resolution, as shown in Fig. 3(f). The CNR value is 41.79. Line pairs in group 2 element 6 with a linewidth of 70.15 μm can be distinguished. Therefore, it is experimentally verified that the proposed method can be applied to realize high-resolution object reconstruction when imaging through dynamic and turbid water with high-randomness light disturbance is conducted.

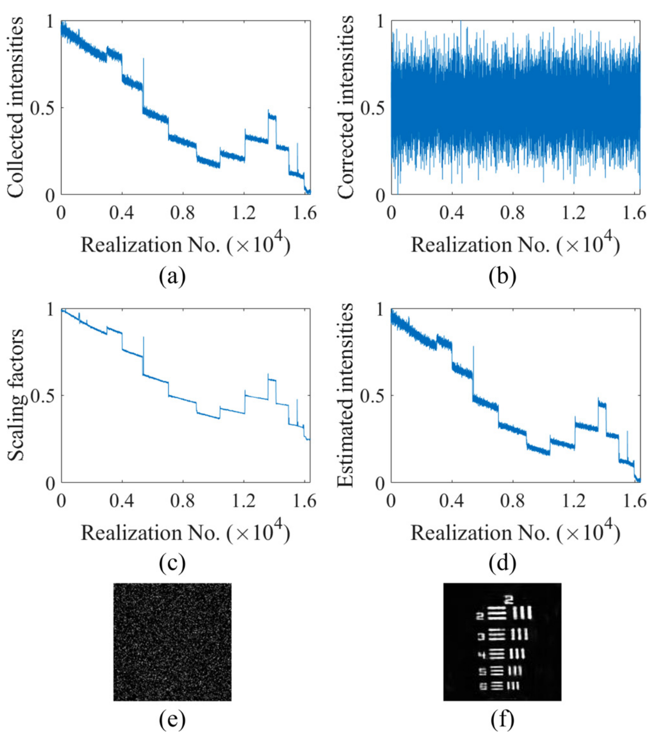

FIG. 3. (a) The single-pixel intensities $\tilde{B}$ experimentally collected in a complex environment, (b)–(d) corrected intensities (realizations), estimated scaling factors, and estimated intensities (realizations) $\hat{B}$ obtained by using the proposed method, (e) ghost reconstruction using DGI, and (f) ghost reconstruction using the proposed method.

To illustrate the robustness, the proposed method is further tested using different objects, i.e., "0," "Y," "U," and "3Lines." The experimentally collected realizations and the recovered results (i.e., corrected realizations, scaling factors, and estimated realizations) by using the proposed method are shown in Fig. S2 in the supplementary material. It can be found that the light disturbance is completely different, similar to variable and unpredictable environments in real-world scenarios. As can be seen in Figs. 4(a)–4(d), reconstruction results using conventional DGI are corrupted by noise and CNR values are $\sim$0. On the contrary, the reconstructed objects using the proposed method are shown in Figs. 4(e)–4(h), with CNR values of 227.25, 229.57, 230.69, and 238.50, respectively. High-contrast objects are retrieved, demonstrating that the developed unified GI framework can accurately infer object information in complex environments. Independent of datasets, the proposed method has high robustness to be generalized to recover different objects and adapt to environmental variety and uncertainty. Ghost reconstruction using the proposed method at different sampling ratios is also studied to reduce the data acquisition burden in complex environments. Experimental results and CNR variations are shown in Figs. S3 and S4 in the supplementary material. It is demonstrated that the proposed method enables high-quality and high-efficiency GI in complex environments with dynamic and turbid water and random light disturbance at a sampling ratio of 6.25%.

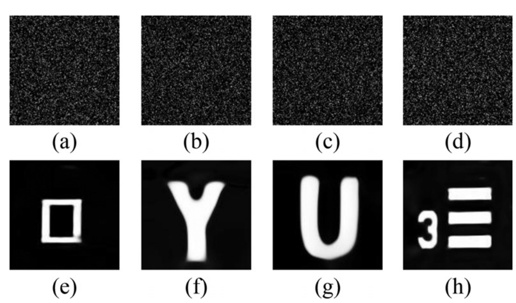

FIG. 4. Ghost reconstruction for the objects "0," "Y," "U," and "3Lines" using (a)–(d) DGI and (e)–(h) the proposed method.

Further investigation of the effect of LED illuminance on the proposed method is carried out at illuminance levels of 6.18, 10.25, 14.12, and 17.89 lux. At different LED illuminance levels, the scaling factors estimated by using the proposed method can always capture environmental variations, and the estimated realizations consistently approximate the experimentally collected realizations (see Fig. S5 in the supplementary material). The typically reconstructed ghost images are shown in Fig. 5. In Figs. 5(a)–5(d), conventional DGI still fails to reconstruct objects owing to the influence of complex environments. In contrast, the proposed method demonstrates high resilience against the harsher environments, as shown in Figs. 5(e)–5(h). The CNR values of the reconstructed object images are 241.68, 238.50, 212.88, and 191.37, respectively. The decrease in the CNR values is attributed to a smaller proportion of effective intensities in the collected realizations at the higher LED illuminance. Despite the decrease, the reconstructed objects always exhibit high visibility. Experimental results verify the robustness of the proposed method against LED illuminance variations. To shorten the acquisition time, the proposed method is feasible to recover high-quality object information in complex environments with different illuminance levels at low sampling ratios (see Figs. S6 and S7 in the supplementary material for details).

To benefit from the characteristics of UNN, a simple and unified framework incorporated with a GI-formation-based physical model is proposed to be applied for optical imaging in complex environments. Since the network structure inherently captures image statistics and impedes noise, the unknown object can be reconstructed with high quality, obviating the requirement for post-processing. Unlike the learning-based method[15] that performs a scaling factor modeling process in a supervised manner, the proposed method does not require datasets and can generate temporally uncorrelated scaling factors. This renders the proposed method to be immune from random environmental variations during experiments and broadens its environmental adaptability. The proposed method can even reconstruct high-quality objects at low sampling ratios, remarkably improving the acquisition efficiency in complex environments compared with previous studies.[14–16]

In conclusion, we have reported a unified GI framework using UNN in complex environments. The proposed method employs two designed networks to respectively estimate the corrected realizations and dynamic scaling factors. Integrating with a GI-formation-based physical model, the network can recover the latent object information with high quality. A series of optical experiments are conducted to verify the effectiveness of the proposed method in complex environments, i.e., dynamic and turbid water with high-randomness light disturbance.

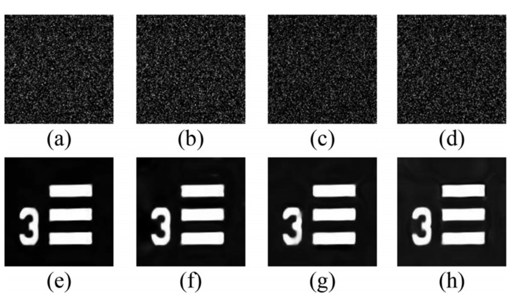

FIG. 5. Ghost reconstruction when LED illuminance is 6.18, 10.25, 14.12, and 17.89 lux, respectively: (a)–(d) DGI and (e)–(h) the proposed method.

Experimental results demonstrate that the proposed method can robustly estimate dynamic scaling factors and realize high-resolution and high-contrast object reconstruction in complex environments, even at low sampling ratios (e.g., 6.25%). The proposed method possesses characteristics of simple integration, broad adaptability, and high efficiency, promoting the advancement in real-world applications of GI.

See the supplementary material for the methods and more experimental results.

This work was supported by the Hong Kong Research Grants Council (Nos. 15224921 and 15223522) and The Hong Kong Polytechnic University (Nos. 1-CDJA and 1-WZ4M).

AUTHOR DECLARATIONS

Conflict of Interest

The authors have no conflicts to disclose.

Author Contributions

Yang Peng: Data curation (equal); Formal analysis (equal); Investigation (equal); Methodology (equal); Writing – original draft (lead). **Wen Chen:** Conceptualization (lead); Formal analysis (lead); Funding acquisition (lead); Methodology (lead); Project administration (lead); Resources (lead); Supervision (lead); Writing – review & editing (lead).

DATA AVAILABILITY

The data that support the findings of this study are available from the corresponding author upon reasonable request.

REFERENCES

[1] T. B. Pittman, Y. H. Shih, D. V. Strekalov, and A. V. Sergienko, "Optical imaging by means of two-photon quantum entanglement," Phys. Rev. A **52**, R3429–3432 (1995).

[2] Z. Zhang, X. Ma, and J. Zhong, "Single-pixel imaging by means of Fourier spectrum acquisition," Nat. Commun. **6**, 6225 (2015).

[3] J. H. Shapiro, "Computational ghost imaging," Phys. Rev. A **78**, 061802 (2008).

[4] F. Ferri, D. Magatti, L. A. Lugiato, and A. Gatti, "Differential ghost imaging," Phys. Rev. Lett. **104**, 253603 (2010).

[5] M. Bina, D. Magatti, M. Molteni, A. Gatti, L. A. Lugiato, and F. Ferri, "Backscattering differential ghost imaging in turbid media," Phys. Rev. Lett. **110**, 083901 (2013).

[6] A. Zhang, Y. He, L. Wu, L. Chen, and B. Wang, "Tabletop x-ray ghost imaging with ultra-low radiation," Optica **5**, 374–377 (2018).

[7] C. Deng, L. Pan, C. Wang, X. Gao, W. Gong, and S. Han, "Performance analysis of ghost imaging lidar in background light environment," Photonics Res. **5**, 431–435 (2017).

[8] P. Janassek, S. Blumenstein, and W. Elsäßer, "Ghost spectroscopy with classical thermal light emitted by a superluminescent diode," Phys. Rev. Appl. **9**, 021001 (2018).

[9] P. Ryczkowski, M. Barbier, A. T. Friberg, J. M. Dudley, and G. Genty, "Ghost imaging in the time domain," Nat. Photonics **10**, 167–170 (2016).

[10] S. Yuan, J. Yao, X. Liu, X. Zhou, and Z. Li, "Cryptanalysis and security enhancement of optical cryptography based on computational ghost imaging," Opt. Commun. **365**, 180–185 (2016).

[11] W. Gong and S. Han, "Correlated imaging in scattering media," Opt. Lett. **36**, 394–396 (2011).

[12]R. E. Meyers, K. S. Deacon, and Y. H. Shih, "Turbulence-free ghost imaging," Appl. Phys. Lett. **98**, 111115 (2011).
[13]L. Zhou, Y. Xiao, and W. Chen, "High-resolution self-corrected single-pixel imaging through dynamic and complex scattering media," Opt. Express **31**, 23027–23039 (2023).
[14]Y. Xiao, L. Zhou, and W. Chen, "High-resolution ghost imaging through complex scattering media via a temporal correction," Opt. Lett. **47**, 3692–3695 (2022).
[15]Y. Peng and W. Chen, "Deep learning-enhanced ghost imaging through dynamic and complex scattering media with supervised corrections of dynamic scaling factors," Appl. Phys. Lett. **124**, 181104 (2024).
[16]Q. Song, Q. Liu, and W. Chen, "High-resolution ghost imaging through dynamic and complex scattering media with adaptive moving average correction," Appl. Phys. Lett. **124**, 211104 (2024).
[17]Y. Gandelsman, A. Shocher, and M. Irani, "'Double-DIP': Unsupervised image decomposition via coupled deep-image-priors," in *Proceedings of the IEEE/CVF Conference on Computer Vision and Pattern Recognition* (IEEE, 2019), pp. 11026–11035.
[18]D. Ren, K. Zhang, Q. Wang, Q. Hu, and W. Zuo, "Neural blind deconvolution using deep priors," in *Proceedings of the IEEE/CVF Conference on Computer Vision and Pattern Recognition* (IEEE, 2020), pp. 3341–3350.
[19]D. Ulyanov, A. Vedaldi, and V. Lempitsky, "Deep image prior," in *Proceedings of the IEEE Conference on Computer Vision and Pattern Recognition* (IEEE, 2018), pp. 9446–9454.
[20]B. Redding, M. A. Choma, and H. Cao, "Speckle-free laser imaging using random laser illumination," Nat. Photonics **6**, 355–359 (2012).